Author Manuscript

Author Manuscript

Author Manuscript

Author Manuscript

HHS Public Access

Author manuscript

Adv Healthc Mater. Author manuscript; available in PMC 2017 March 01.

Published in final edited form as:

Adv Healthc Mater. 2016 March ; 5(6): 711–719. doi:10.1002/adhm.201500553.

Flexible pH-Sensing Hydrogel Fibers for Epidermal Applications

Dr. Ali Tamayol[*],
Biomaterials Innovation Research Center, Department of Medicine, Brigham and Women's Hospital, Harvard Medical School, Cambridge, MA 02139, USA. Harvard-MIT Division of Health Sciences and Technology, Massachusetts Institute of Technology, Cambridge, MA 02139 USA

Dr. Mohsen Akbari[*],
Biomaterials Innovation Research Center, Department of Medicine, Brigham and Women's Hospital, Harvard Medical School, Cambridge, MA 02139, USA. Harvard-MIT Division of Health Sciences and Technology, Massachusetts Institute of Technology, Cambridge, MA 02139 USA. Wyss Institute for Biologically Inspired Engineering, Harvard University, Boston, MA, 02115, USA

Dr. Yael Zilberman[*],
Nanoscale Integrated Sensors and Circuits Laboratory (Nanolab), Department of Electrical and Computer Engineering, Tufts University, Medford, MA, 02155, USA. Department of Biomedical Engineering, Tufts University, Medford, MA, 02155, USA

Mr. Mattia Comotto,
Biomaterials Innovation Research Center, Department of Medicine, Brigham and Women's Hospital, Harvard Medical School, Cambridge, MA 02139, USA. Harvard-MIT Division of Health Sciences and Technology, Massachusetts Institute of Technology, Cambridge, MA 02139 USA

Mr. Emal Lesha,
Biomaterials Innovation Research Center, Department of Medicine, Brigham and Women's Hospital, Harvard Medical School, Cambridge, MA 02139, USA. Harvard-MIT Division of Health Sciences and Technology, Massachusetts Institute of Technology, Cambridge, MA 02139 USA

Mr. Ludovic Serex,
Biomaterials Innovation Research Center, Department of Medicine, Brigham and Women's Hospital, Harvard Medical School, Cambridge, MA 02139, USA. Harvard-MIT Division of Health Sciences and Technology, Massachusetts Institute of Technology, Cambridge, MA 02139 USA

Dr. Sara Bagherifard,
Biomaterials Innovation Research Center, Department of Medicine, Brigham and Women's Hospital, Harvard Medical School, Cambridge, MA 02139, USA. Harvard-MIT Division of Health Sciences and Technology, Massachusetts Institute of Technology, Cambridge, MA 02139 USA. Department of Mechanical Engineering, Politecnico di Milano, Milan 20156, Italy

Ms. Yu Chen,

Correspondence to: Ali Khademhosseini.

[*]A. Tamayol, M. Akbari, and Y. Zilberman contributed equally to this work.

The authors declare no conflict of interests in this work.

Author Manuscript Author Manuscript Author Manuscript Author Manuscript

Nanoscale Integrated Sensors and Circuits Laboratory (Nanolab), Department of Electrical and Computer Engineering, Tufts University, Medford, MA, 02155, USA. Department of Biomedical Engineering, Tufts University, Medford, MA, 02155, USA

Mr. Guoqing Fu,
Nanoscale Integrated Sensors and Circuits Laboratory (Nanolab), Department of Electrical and Computer Engineering, Tufts University, Medford, MA, 02155, USA. Department of Biomedical Engineering, Tufts University, Medford, MA, 02155, USA

Ms. Shideh Kabiri Ameri,
Nanoscale Integrated Sensors and Circuits Laboratory (Nanolab), Department of Electrical and Computer Engineering, Tufts University, Medford, MA, 02155, USA. Department of Biomedical Engineering, Tufts University, Medford, MA, 02155, USA

Mr. Weitong Ruan,
Nanoscale Integrated Sensors and Circuits Laboratory (Nanolab), Department of Electrical and Computer Engineering, Tufts University, Medford, MA, 02155, USA. Department of Biomedical Engineering, Tufts University, Medford, MA, 02155, USA

Mr. Eric L. Miller,
Nanoscale Integrated Sensors and Circuits Laboratory (Nanolab), Department of Electrical and Computer Engineering, Tufts University, Medford, MA, 02155, USA. Department of Biomedical Engineering, Tufts University, Medford, MA, 02155, USA

Dr. Mehmet R. Dokmeci,
Biomaterials Innovation Research Center, Department of Medicine, Brigham and Women's Hospital, Harvard Medical School, Cambridge, MA 02139, USA. Harvard-MIT Division of Health Sciences and Technology, Massachusetts Institute of Technology, Cambridge, MA 02139 USA. Wyss Institute for Biologically Inspired Engineering, Harvard University, Boston, MA, 02115, USA

Prof. Sameer Sonkusale, and
Nanoscale Integrated Sensors and Circuits Laboratory (Nanolab), Department of Electrical and Computer Engineering, Tufts University, Medford, MA, 02155, USA

Prof. Ali Khademhosseini
Biomaterials Innovation Research Center, Department of Medicine, Brigham and Women's Hospital, Harvard Medical School, Cambridge, MA 02139, USA. Harvard-MIT Division of Health Sciences and Technology, Massachusetts Institute of Technology, Cambridge, MA 02139 USA. Wyss Institute for Biologically Inspired Engineering, Harvard University, Boston, MA, 02115, USA. Department of Physics, King Abdulaziz University, Jeddah 21569, Saudi Arabia. Department of Bioindustrial Technologies, College of Animal Bioscience and Technology, Konkuk University, Seoul, Republic of Korea

Ali Tamayol: alik@rics.bwh.harvard.edu

Abstract

Epidermal pH is an indication of the skin's physiological condition. For example, pH of wound can be correlated to angiogenesis, protease activity, bacterial infection, etc. Chronic non-healing wounds are known to have an elevated alkaline environment, while healing process occurs more readily in an acidic environment. Thus, dermal patches capable of continuous monitoring of pH

Author Manuscript Author Manuscript Author Manuscript Author Manuscript

can be used as point-of-care systems for monitoring skin disorder and the wound healing process. Here, we present pH-responsive hydrogel fibers that can be used for long-term monitoring of epidermal wound condition. We load pH-responsive dyes into mesoporous microparticles and incorporate them into hydrogel fibers developed through microfluidic spinning. The fabricated pH-responsive microfibers are flexible and can create conformal contact with skin. The response of pH-sensitive fibers with different compositions and thicknesses are characterized. The suggested technique is scalable and can be used to fabricate hydrogel based wound dressing with a wide range of sizes. Images of the pH-sensing fibers during real-time pH measurement can be captured with a smart phone camera for convenient readout on-site. Through image processing, a quantitative pH map of the hydrogel fibers and the underlying tissue can be extracted. The developed skin dressing can act as a point-of-care device for monitoring the wound healing process.

Keywords

pH monitoring; Wound healing; Luminescence; Hydrogel fibers; Microfluidic spinning

Introduction

Skin disorders such as chronic wounds have a high prevalence and affect a large population [1]. Wound healing is a complex, multifaceted process which is influenced by both intrinsic and extrinsic factors [2]. Wound is a dynamic environment, thus, monitoring different physicochemical and physiological parameters provides information on its status [3]. The pH of healthy skin is slightly acidic (pH=4–6) but becomes more alkaline when the barrier is breached and the internal body fluids reach the wounded area[4]. During the healing process, the pH of the wound shifts towards neutral and becomes acidic after complete healing [5]. The wound pH influences various factors including oxygen delivery, angiogenesis, protease activity, and bacterial infection. Oxygen delivery at lower pH environments, particularly in chronic wounds is reported to promote healing [6]. Wound pH also alters activity of enzymes that can collectively degrade most of the extracellular matrix (ECM) compounds [7]. Extremely acidic pH values can represent a bacterial infection [8]. Thus, continuous monitoring of the skin pH is of great importance.

During the past decade, several research groups have developed pH sensors that can continuously monitor the skin condition [4]. One of the main characteristics of these sensors is that they should form a conformal contact with the skin and do not restrain the skin movement. As a result, their mechanical characteristics should match those of native skin. Existing pH sensors are mostly either electrochemical or calorimetric [4, 9, 10]. Electrochemical sensors measure the concentration of H^+ ions through measuring the rate of electrochemical reactions [10]. Recent advances in the field of flexible electronics and biomaterials have enabled the fabrication of epidermal sensors that are flexible and wearable [11]. These sensors are mostly fabricated on elastic biocompatible substrates with biomimetic mechanical characteristics [12]. The substrate also separates the fabricated sensors from direct contact with skin to eliminate the chance of irritation[3]. However, as the wound exudate and sweat are rich with various proteins and chemokines, these epidermal

Author Manuscript Author Manuscript Author Manuscript Author Manuscript

electrochemical sensors are susceptible to degradation and electrode poisoning, which may affect their sensitivity and output over time [13]. In addition, electrochemical systems require the integration of electronic circuitry and power source for analysis of their readout.

Another approach that has attracted noticeable attention is the use of pH sensitive materials and luminescent dyes for detection of skin pH [14]. These colorimetric sensors are robust and easy-to-read and can be utilized without integrated electronics. However, a key challenge for fabrication and use of luminescence systems is to prevent the dye from leaching out of the dressing onto the skin. In addition, the sensitivity of the dye should cover the entire range of pH variation observed in skin disorders and wounds (pH: 4–9).

Hydrogels are formed from a hydrophilic network of polymers and that can uptake high amounts of water and exudates [15]. They are also typically transparent, which makes them suitable for the development of luminescence-based diagnostics. The high water content of hydrogel helps with the maintenance of skin and wound humidity that is an important factor for enhancing the healing process [16]. Thus, hydrogels are promising candidates for use as substrate in luminescence based systems. The key challenge is to create thin hydrogels constructs that are flexible and can form a conformal contact with the skin. Alginate is a natural hydrogel that has been extensively used in the literature due to its mechanical strength and ease-of-fabrication [17]. Alginate microfibers, which are inherently flexible and can be shaped into irregular geometries, are attractive materials for long term monitoring of wound condition [18]. These microfibers can be assembled using bioprinting and textile techniques to create gas and exudates permeable constructs with suitable mechanical properties [19]. Another challenge for use of hydrogel constructs in luminescence based systems is their large pore sizes, which allows the entrapped dye to escape.

Here, we fabricated alginate-based microfibers loaded with pH-responsive beads for long-term monitoring the epidermal pH level (Figure 1a). Mesoporous silica beads were loaded with pH sensitive dye and consequently embedded in the hydrogel microfibers. The fabricated pH-sensors were flexible and could be assembled into a wearable patch. Encapsulation of the beads within the hydrogel fibers prevents the beads from dispersing in the wound area while providing a biocompatible interface with the wound site. Images captured using a smart phone alone, without the need for any expensive instrumentation for optical readout, is used to determine pH values from the engineered wearable patches. These pH sensitive fibers can be added to any commercial wound dressing to provide real-time information about the wound condition without the need for expensive instrumentation.

Results and Discussions

The alginate-based fibers containing pH-sensitive mesoporous silica beads were fabricated in a co-axial flow microfluidic device made from pulled capillaries as described in the materials and methods (Figure 1b). Briefly, sodium-alginate (2% w/v) mixed with the desired concentration of glycerol (0%–60% w/v) and bead density (0–0.5 million/mL) was injected through the core channel. A sheath flow of $CaCl_2$ (2% w/v) was formed around the core prepolymer stream to chemically crosslink the alginate and to continuously produce hydrogel-fibers. After gelation, the fibers were thoroughly washed by DI water to remove

Author Manuscript Author Manuscript Author Manuscript Author Manuscript

the excess calcium solution and uncrosslinked polymers. Alginate was selected as it is an approved material for epidermal applications and has excellent biocompatibility and mechanical properties. Additionally, calcium alginate is a natural hemostat that can be removed from the wound site without much trauma and discomfort [20]. Glycerol is a well-known plasticizer that has been widely used to improve the mechanical properties and flexibility of biomaterials used for epidermal patches and food packaging [21]. The fabricated fibers finely responded to any variations in the pH of the solution by changing color from dark red (basic) to yellow (acidic), enabling colorimetric measurement (Figure 1b–i).

The use of co-axial flow in the microfluidic setting enabled controlling the diameter of the fabricated hydrogel microfibers. We varied the core flow rate in the range of 50–800 $\mu L.min^{-1}$ and measured the diameter of the fabricated fibers at two different $CaCl_2$ flow rates of 2 mL/min and 5 mL/min. As expected, the fiber diameter increased with enhancing the core flow rate (Figure 1c) spanning from 200 to 1000 μm. Variation of the fiber diameter with respect to the core flow rate was less pronounced when higher $CaCl_2$ flow rates were used; allowing for fine tuning of the fiber diameter. Figure 1d shows the effect of the density of loaded beads on the diameter of microfibers. Beads at densities ranging from $0–1\times10^5$ beads/mL were mixed with the prepolymer solutions and injected into the core channel. Low bead densities showed insignificant affect on the fiber diameter, while using higher bead densities led to a 25% increase in the fiber diameter (at 10^5 beads/mL). This change may be attributed to the momentum of beads leaving the middle channel which has led to their diffusion in the $CaCl_2$ stream.

Figure 2 summarizes the physical properties of the fabricated pH-sensitive fibers. The visual appearance of the fibers when loaded with different bead densities is shown in Figure 2a. Fibers loaded with high bead densities were clearly visible by naked eyes, whereas the alginate fibers were transparent. Effect of encapsulating the beads at different densities on the mechanical properties of the fibers is shown in Figure 2b. Our results suggest that adding more beads to the polymer led to stiffer fibers evidenced by higher elastic modulus. This enhancement in elastic modulus has been previously reported in hybrid hydrogels containing stiff particles [22]. The high surface area results in the infiltration of the gel in the pores of the particles which will induce mechanical interlocking between the particles and the hydrogel matrix. The pertinent literature suggests a reduction in the elastic limit and ultimate strain by incorporation of particles unless there is an electrostatic interaction between the particles and the hydrogel. The mesoporous particles are positively charged while alginate is negative thus it is expected that the effect of particles on the elastic modulus to be less pronounced. Similarly, our experiments revealed a slight reduction in the ultimate strain of the fabricated fibers containing microbeads especially at the highest concentration. We analyzed the influence of glycerol content on the Young's modulus of the fabricated fibers immediately after fabrication (fresh) and when dried for 24 hrs (Figure 2c). Glycerol was observed to have insignificant effect on the Young's modulus of the fibers. However, when dried for 24 hrs, the fibers made from glycerol alginate blends showed higher mechanical properties while pure alginate fibers were fragile and could not withstand tensile loading.

Author Manuscript Author Manuscript Author Manuscript Author Manuscript

One of the main advantages of using hydrogels as a substrate for epidermal applications is their ability to maintain the moist environment of the wound. However, microfibers with high volume to surface ratio are prone to rapid dehydration. Dehaydration rate of fibers made from pure alginate and hybrid alginate/glycerol is shown in Figure 2c. Both alginate and glycerol/alginate fibers lost their water content, but the process was slower in the blend hydrogels due to hygroscopic characteristics of glycerol. Pure alginate fibers became brittle, whereas the fibers made from the hybrid alginate/glycerol remained flexible and mechanically stable after dehydration (Figure 2d). Although alginate-based hydrogels have a considerable water uptake capacity[23], due to the small volume of the generated fibers they offer limited water uptake.

We evaluated the biocompatibility of the pH-sensitive fibers by placing them in cell culture wells containing human-derived keratinocytes, the predominant cell type in the epidermis. Cells and fibers with different compositions with and without pH-responsive beads were cultured for 7 days and the metabolic activity of the cells were monitored as an indicator of their viability and proliferation (Figure 2e). Our results did not show any significant variation in cellular activity due to presence of glycerol and pH-responsive beads. (Figure 2e). The toxicity of the beads corresponded to the leakage of the pH-sensitive dye residues from the fibers. Figure S1 shows a fluorescent micrograph of the cells F-actin and nuclei stained in green and blue, respectively. Normal cellular morphology was preserved during their culture against hydrogel fibers containing pH-responsive beads.

To assess the sensitivity of the fibers' response to variation in the pH of the environment, pH sensing microfibers were placed in a polydimethylsiloxane (PDMS) chamber (Figure 3a). The chamber had an inlet and an outlet that could be connected to a peristatic pump. Solutions with different pH values were introduced continuously into the channel using a peristatic pump and the variation in the color of the fibers was analyzed using a USB spectrophotometer. Each solution was continuously flowed for at least 30 min to ensure stabilized response of the fibers. Figure 3b shows different colors of the pH-responsive fibers at solutions with pH values of 6.5 (yellow) and 8 (red). Figure s2 shows an example of the step response of 570 μm fiber to different pH solutions, ranging from 6.5 to 9 and vise versa. The normalized intensity change (I corresponds to intensity and I_b corresponds to the baseline intensity at zero time) over time for 600 nm wavelength, which representing the decrease in intensity with an increase in the pH.

The effect of fiber diameter on the response time and transmittance change of fibers (Figure 3b) was also studied. The response time was extracted from the slope of intensity change during exposure to solutions with different pH values, so large slope will results in fast response time and vice versa. With the exception of the fibers with 800 μm in diameter, overall the response time increased with the fiber size, as expected. However, the fibers with 800μm diameter demonstrated better performance in terms of response time and durability than thinner fibers over time. This quick response of fibers with 800μm might be due to the higher number of encapsulated responsive microbeads distributed in the periphery of the fiber. The response magnitude (ΔT) for different fiber diameters was also tested at a range of pH environments of 6.5 to 9 (Figure 3d). The 800μm fiber also showed the highest response magnitude in comparison to the two other fibers (570μm and 600μm). Note that these two

Author Manuscript Author Manuscript Author Manuscript Author Manuscript

fibers, although they have different condition in fabrication (different alginate flow rate; 2μl/min and 3μl/min), are similar in diameter, which leads to similar results in terms of both response time and magnitude (Figure 3d). According to the optical and mechanical results, the applicative fabricated fibers that was used throughout the analysis in this paper was 800μm diameter fibers made of alginate mixed with 20% (v/v) glycerol.

The use of smart phones forgoes the need for expensive instrumentation and allows these fibers to be read out at point of care to monitor epidermal pH. Therefore, the feasibility of using smart phones for measuring the pH by taking images and processing them off line was evaluated. We placed the fibers in a PDMS well and filled them with different pH values. Figure 4a shows the variation in colors of the brilliant yellow dye-based fibers at pH=6 (yellow) and pH=8 (red). Images were taken using a smart phone and were used to determine the pH. To calibrate the imaging system, the pH-sensing fibers were immersed in different pH solutions (pH=6, 6.5, 7, 7.5, 8, and 9) at room temperature, and photos were taken after 30 minutes using the smart phone camera. The pH sensing results were extracted from the images taken by the smart phone and processes using homemade MATLAB code. A typical example of raw data extracted from the images over time is shown in Figure S3. The figure shows the RGB signal over time at different pH environments ranging from 6.5 to 9. Then, the raw data was further processed and RGB magnitudes and fitting curve with correlated equation for determination of actual pH were designed using a homemade MATLAB code. Images were taken over time to determine the rate of variation in the fiber color at different pH values. Figure 4b and c show an example of the RGB (red, green, blue) response magnitude and the flitting curve and corresponded equation for determination of the actual pH value from the RGB values, respectively. In this case, the best fitting was correlated to the R value solely. The results showed continuous RGB intensity change when transferring pH-sensing fiber from one pH solution to another. Figure 4d shows the response time of fibers with different diameters captured using a smart phone. The response time was counted from the moment the fiber was immersed in pH solution until its color was finally stabilized. The 800μm fiber showed the fastest response time, which was in agreement with data obtained from the spectrophotometer. We used the RGB values extracted from the image as references to generate correlations for pH versus R, G and B channels, which can be used later for real-time pH monitoring. Most of fibers show monotonic alterations over pH with R, G or B, or the combinations of two.

The pH-responsive fibers were fabricated using the microfluidic platform and then were attached to a transparent medical tape, which created a wearable platform (Figure 5). The prepared patches were placed on explanted pig skin and agarose gel sprayed with different pH solutions (pH=5.2, 6.2, 7.2, and 8.2) and photos were taken using a smart phone after 30 minutes, when the fiber colors were stable (Figure 5a,b and Figure S2). The insets in Figure 5a show the micrograph of the fibers at different pH values. The images were then processed by an in-house Matlab code and the RGB values were determined and compared to the correlations described in Figure 4. Thus, the real-time values of sprayed pig skin pH could be determined. The extracted pH values were 5.69, 6.26, 7.38 and 8.13, which were in reasonable agreement with the actual pH of the sprayed pig skin samples (5.2, 6.2, 7.2 and 8.2 respectively in Figure 5d). The size and number of fibers could also be adjusted as shown in Figure 5d.

Author Manuscript Author Manuscript Author Manuscript Author Manuscript

Conclusions

We developed hydrogel microfibers containing mesoporous particles loaded with a pH-responsive dye. The alginate-based microfibers were generated using the microfluidic spinning method that enabled controlling the size of the fabricated fibers. The fabricated pH-responsive microfibers were flexible and could maintain conformal contact with skin. In addition, the electrostatic interactions between the dye and mesoporous particles minimized the leach out of dye from fibers. The response time and sensitivity of pH-sensitive fibers with different compositions and thicknesses were characterized. In addition, we assembled on a transparent medical tape to form a pH-responsive wound dressing. Images of the pH-sensing fibers during real-time pH measurement were captured with a smart phone camera for convenient readout on-site. Thus, the developed skin dressing could be used as a point of care device for monitoring the wound healing process. We think that with the recent advances in fabrication and assembly of hydrogel fibers, highly porous and oxygen permeable wet wound dressings that can map the pH of chronic wounds can be manufactured. Clinical validation of the smart multi-functional wound dressing on wounded pigskin is currently underway.

Experimental Section

Materials

Sodium alginate, calcium chloride ($CaCl_2$), agarose, brilliant yellow dye, and resin microbeads powder were purchased from Sigma Aldrich (St. Louis, MO, USA). Dulbecco's modified Eagle medium (DMEM), fetal bovine serum (FBS), 0.05% trypsin-EDTA (1X), and antibiotics (Penicillin/Streptomycin) were purchased from Invitrogen (Carlsbad, CA, USA). PrestoBlue® Cell Viability Reagent was obtained from Life Technologies.

Fabrication of pH-responsive microbeads

The responsive beads preparation and the ratio between the dye and the beads are based on our previous work [24]. Briefly, the pH-responsive dye was prepared by first dissolving 22.5 mg of brilliant yellow dye in 1 mL of ethanol (>99.5%, Sigma–Aldrich) followed by adding of 4 mL of deionized water. Subsequently, 563 mg of anion exchange resin microbeads powder and 5 mL of deionized water were added to the dye solution and stirred for 1 hr at room temperature using a magnetic stirrer. The ionic interaction between the brilliant yellow dye and the beads resulted in the dye encapsulation. The saturation of the ionic interactions between the negatively charged dye and the positively charged beads cause the dye excess to be free in the solution. The colored beads were filtered and diluted again in fresh DI water. The dye-beads loading process was reproducible and hence the RGB values extracted from the images were consistent.

Fabrication of hydrogel fibers

The solution of alginate and glycerol was mixed with pH-responsive beads. The mixture was then loaded into a 1 mL plastic syringe (BD Biosciences) and was connected to a syringe pump (Harvard Apparatus PHD 4400, Holliston, MA, USA). The syringe was connected using chemical resistant clear PVC tubing to a PDMS-based microfluidic chip. A cylindrical

Author Manuscript Author Manuscript Author Manuscript Author Manuscript

pulled capillary tube was coaxially aligned within a channel fabricated in the PDMS device. The inner diameters of the injection tube and PDMS channel were ~200 μm and 820 μm, respectively. The microfluidic chip was capable of creating core shell stream of the pre-polymer as the core and 2% (w/v) $CaCl_2$ as the sheath. The fabricated fibers were then collected into a small beaker filled with $CaCl_2$ solution. The fabrication of the fibers and their size variation were monitored using an inverted optical microscope (TE2000-U, Nikon).

Dehydration test

To assess the weight loss of different hydrogel compositions, circular disks of the hydrogel (1 mm thick and 8 mm in diameter) were fabricated. Briefly, the prepolymer was poured in a mold and was covered with a sheet of agarose (2% w/v) containing a $CaCl_2$ solution (2% w/v). The samples were left for 20 min to crosslink and then were 2% w/v $CaCl_2$ solution. Immediately following their fabrication, samples were weighted and placed inside an incubator at 37 °C. At definite time intervals, samples were weighted and the weight loss was calculated considering the initial value. Dehydration test was continued for 72 hr.

Mechanical test

The mechanical properties of the prepared fibers with different compositions and bead concentration were measured using an Instron 5542 mechanical tester (Norwood, MA, USA) with a 1 KN load cell following the method used to measure the mechanical properties of GelMA and other hydrogels [25]. The sample was glued to two clamps to avoid slipping and stretched at a constant clamp displacement rate of 0.5 mm/min. The tensile properties of samples including elastic modulus (the tangent slope of the linear section of the stress-strain curve) were determined.

Characterization of response to pH variation

The pH-sensing fibers were fabricated and cut to identical length using a razor. A 25 mm wide, 75 mm long, and 1mm chamber was created in PDMS. The PDMS piece was then bonded to a glass slide. The fibers were aligned and fixed in the chamber (See Figure 3a).

The response of the aligned fiber to different pH environments was also characterized by USB spectrometer. The device was covered using PDMS microfluidic channels to allow continuous flowing of different pH (pH=5.5, 6, 6.5, 7, 7.5, 8, 9) solutions. Each pH solution was flown for 30 minutes and the change in the color was monitored at different wavelengths over time.

For smart phone measurement, the align fibers- based device was immersed at different pH solution (pH=5.5, 6.5, 7.4, 8 and 9) and photos were taken after 30 minutes, when the color of fiber was stable and further processed in MATLAB. Each image taken by cell phone contained certain amount of pixels, and each pixel was composed of three R, G and B components. The magnitude of RGB varied from 0 to 255 for each pixel. Different colors were represented by the combination of unique RGB values, which can be extracted separately in MATLAB. Since the fibers in different pH environments have different colors, so that the magnitude of each RGB components also varies. This variation trend was

Author Manuscript Author Manuscript Author Manuscript Author Manuscript

extracted and used for pH identification. However, it was found that only R value changed monotonically with pH variation, thus the equation of pH as a function of R was extracted by the fibers in these reference photos and was used for pH extraction of samples.

It should be noted that the color of digital photos taken by a smart phone was significantly different from the real color of the object. Considering this fact, standard white/black/red/green/blue color paper strips were added to each sample for calibration purpose. The RGB intensity variation of those standard color strips was used to compensate for the subtle differences in the pictures taken by a smart phone under different lighting conditions. This variation information is measured and processed to calibrate the colorimetric information acquired from beads in each picture. By doing so, the more accurate or "real" RGB values of the beads in each sample can be obtained and therefore more accurate pH result can be read.

Characterization of assembled patch

In the assembled patch experiment, the fiber bandages were attached to pig skin and solutions with pH equals to 5.2, 6.2, 7.2 and 8.2 are applied to pig skin respectively. After taking photos of all the fiber bandages on pH modified- pig skin, the R values for the fiber pixels in each pH environment are extracted. Then these R values were fit in the previously attained R as a function of pH formula, thus their corresponding pH values can be calculated. It is worth noting that the RGB values extraction process for fibers in each reference and sample photos were calibrated for background variation dues to different illumination conditions.

Cell studies

Keratinocytes were cultured in a medium composed of DMEM, 10% FBS, and 1% penicillin/streptomycin. Cells were used after ~80% confluency.

For cytotoxicity assessment, cells were seeded at the concentration of 5×10^3 cells per well in 24-well polystyrene plates. Hydrogel fibers with and without beads were placed into the wells and cellular metabolic activity was measured using PrestoBlue® assay according to manufacturer protocol. PrestoBlue® reagent was uptaken by viable cells and reduced to a fluorescing stain. The fluorescent intensity was used as a measure of cellular metabolic activity. The assay was performed on days 1, 3 and 7 and the fluorescent intensity was measured using a BioTek UV/vis Synnergy 2 microplate reader.

Supplementary Material

Refer to Web version on PubMed Central for supplementary material.

Acknowledgments

SB acknowledges funding from MIT-Italy program (Progetto Rocca) and Polimi International Fellowship (PIF). AK, MRD and AT acknowledge funding from the National Science Foundation (EFRI-1240443), the office of Naval Research Young National Investigator Award, and the National Institutes of Health (HL092836, DE019024, EB012597, AR057837, DE021468, HL099073, EB008392).

Author Manuscript Author Manuscript Author Manuscript Author Manuscript

References

1. Fonder MA, Lazarus GS, Cowan DA, Aronson-Cook B, Kohli AR, Mamelak AJ. Journal of the American Academy of Dermatology. 2008; 58:185. [PubMed: 18222318] Mustoe TA, O'Shaughnessy K, Kloeters O. Plastic and Reconstructive Surgery. 2006; 117:35S. [PubMed: 16799373]
2. Falanga V. The Lancet. 366:1736.Broughton G 2nd, Janis JE, Attinger CE. Plastic and Reconstructive Surgery. 2006; 117:12S. [PubMed: 16799372]
3. Huang X, Liu Y, Chen K, Shin WJ, Lu CJ, Kong GW, Patnaik D, Lee SH, Cortes JF, Rogers JA. Small. 2014; 10:3083. [PubMed: 24706477]
4. Dargaville TR, Farrugia BL, Broadbent JA, Pace S, Upton Z, Voelcker NH. Biosensors and Bioelectronics. 2013; 41:30. [PubMed: 23058663]
5. Tsukada K, Tokunaga K, Iwama T, Mishima Y. Wounds. 1992; 4:16.
6. Leveen HH, Falk G, Borek B, Diaz C, Lynfield Y, Wynkoop BJ, Mabunda GA, Rubricius JL, Christoudias GC. Annals of surgery. 1973; 178:745. [PubMed: 4759406] Gordillo GM, Sen CK. The American journal of surgery. 2003; 186:259. [PubMed: 12946829]
7. Greener B, Hughes A, Bannister N, Douglass J. Journal of wound care. 2005; 14:59. [PubMed: 15739652]
8. Schneider LA, Korber A, Grabbe S, Dissemond J. Archives of dermatological research. 2007; 298:413. [PubMed: 17091276]
9. Sharp D. Biosensors and Bioelectronics. 2013; 50:399. [PubMed: 23893062] Hattori Y, Falgout L, Lee W, Jung SY, Poon E, Lee JW, Na I, Geisler A, Sadhwani D, Zhang Y, Su Y, Wang X, Liu Z, Xia J, Cheng H, Webb RC, Bonifas AP, Won P, Jeong JW, Jang KI, Song YM, Nardone B, Nodzenski M, Fan JA, Huang Y, West DP, Paller AS, Alam M, Yeo WH, Rogers JA. Advanced Healthcare Materials. 2014; 3:1597. [PubMed: 24668927]
10. Ochoa M, Rahimi R, Ziaie B. Biomedical Engineering, IEEE Reviews in. 2014; 7:73.
11. Kim D-H, Lu N, Ma R, Kim Y-S, Kim R-H, Wang S, Wu J, Won SM, Tao H, Islam A, Yu KJ, Kim T-i, Chowdhury R, Ying M, Xu L, Li M, Chung H-J, Keum H, McCormick M, Liu P, Zhang Y-W, Omenetto FG, Huang Y, Coleman T, Rogers JA. Science. 2011; 333:838. [PubMed: 21836009] Yeo WH, Kim YS, Lee J, Ameen A, Shi L, Li M, Wang S, Ma R, Jin SH, Kang Z, Huang Y, Rogers JA. Advanced Materials. 2013; 25:2773. [PubMed: 23440975]
12. Najafabadi AH, Tamayol A, Annabi N, Ochoa M, Mostafalu P, Akbari M, Nikkhah M, Rahimi R, Dokmeci MR, Sonkusale S, Ziaie B, Khademhosseini A. Advanced Materials. 2014; 26:5823. [PubMed: 25044366]
13. Wencel D, Abel T, McDonagh C. Analytical Chemistry. 2014; 86:15. [PubMed: 24180284]
14. Schreml S, Meier RJ, Wolfbeis OS, Landthaler M, Szeimies RM, Babilas P. Proceedings of the National Academy of Sciences. 2011; 108:2432.
15. Annabi N, Tamayol A, Uquillas JA, Akbari M, Bertassoni LE, Cha C, Camci-Unal G, Dokmeci MR, Peppas NA, Khademhosseini A. Advanced Materials. 2014; 26:85. [PubMed: 24741694]
16. Jones A, Vaughan D. Journal of Orthopaedic Nursing. 2005; 9(Supplement 1):S1.
17. Knill CJ, Kennedy JF, Mistry J, Miraftab M, Smart G, Groocock MR, Williams HJ. Carbohydrate Polymers. 2004; 55:65.Tamayol A, Najafabadi AH, Aliakbarian B, Arab-Tehrany E, Bertassoni L, Annabi N, Akbari M, Juncker D, Khademhosseini A. Advanced Healthcare Materials. 2015 Accepted.
18. Akbari M, Tamayol A, Laforte V, Annabi N, Najafabadi AH, Khademhosseini A, Juncker D. Advanced Functional Materials. 2014; 24:4060. [PubMed: 25411576] Heo YJ, Shibata H, Okitsu T, Kawanishi T, Takeuchi S. Proceedings of the National Academy of Sciences. 2011; 108:13399.
19. Riahi R, Tamayol A, Shaegh SAM, Ghaemmaghami AM, Dokmeci MR, Khademhosseini A. Current Opinion in Chemical Engineering. 2015; 7:101.Tamayol A, Akbari M, Annabi N, Paul A, Khademhosseini A, Juncker D. Biotechnology Advances. 2013; 31:669. [PubMed: 23195284]
20. Paul W, Sharma CP. Trends Biomater Artif Organs. 2004; 18:18.
21. Lavorgna M, Piscitelli F, Mangiacapra P, Buonocore GG. Carbohydrate Polymers. 2010; 82:291.Patel, HA. Google Patents. 1995.

Author Manuscript Author Manuscript Author Manuscript Author Manuscript

22. Sa V, Kornev KG. Carbon. 2011; 49:1859.
23. Tamayol A, Najafabadi AH, Aliakbarian B, Arab-Tehrany E, Akbari M, Annabi N, Juncker D, Khademhosseini A. Advanced Healthcare Materials. 2015 n/a.
24. Zilberman Y, Chen Y, Sonkusale SR. Sensors and Actuators B: Chemical. 2014; 202:976.Chen Y, Zilberman Y, Mostafalu P, Sonkusale SR. Biosensors and Bioelectronics. 2015; 67:477. [PubMed: 25241151]
25. Chen YC, Lin RZ, Qi H, Yang Y, Bae H, Melero-Martin JM, Khademhosseini A. Advanced Functional Materials. 2012Annabi N, Tsang K, Mithieux SM, Nikkhah M, Ameri A, Khademhosseini A, Weiss AS. Advanced Functional Materials. 2013

Author Manuscript Author Manuscript Author Manuscript Author Manuscript

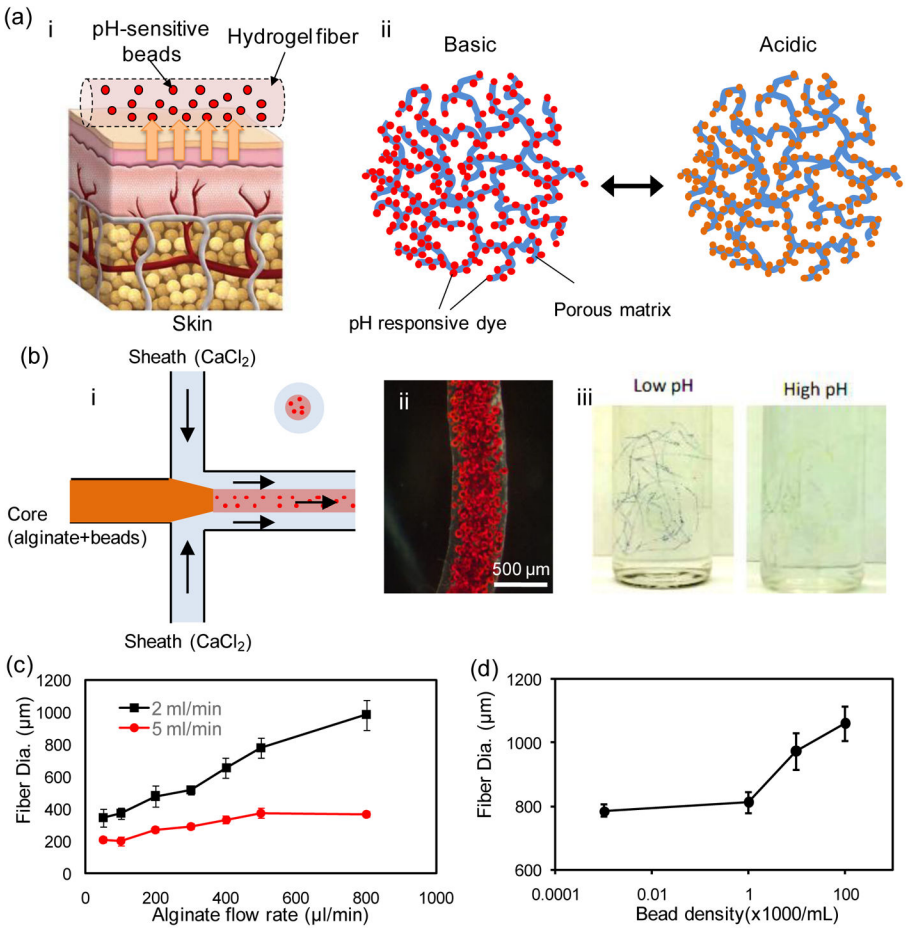

Figure 1.

Fabrication of pH-sensing microfibers. (a) A schematic illustration of the pH-sensing hydrogel microfiber designed for long-term epidermal monitoring (i) and the action mechanism of the mesoporous silica particles containing pH-responsive dye with electrostatic interaction to the solid matrix of the mesoporous particles (ii). (b) Schematic of the fiber fabrication process using coaxial streams of Na-alginate mixed with dye loaded beads surrounded with $CaCl_2$ solution (i). A typical bead-laden alginate fiber fabricated using the microfluidic chip (ii). A representative micrograph of pH-responsive bead-laden hydrogel microfibers (iii). (c) Effect of core flow rate on the fiber diameter at two $CaCl_2$ flow rates of 2 and 5 mL/min. (d) Effect of the bead density on fiber diameter; the core and sheath flow rates were constant at 600 μL/min and 2 mL/min, respectively.

Author Manuscript Author Manuscript Author Manuscript Author Manuscript

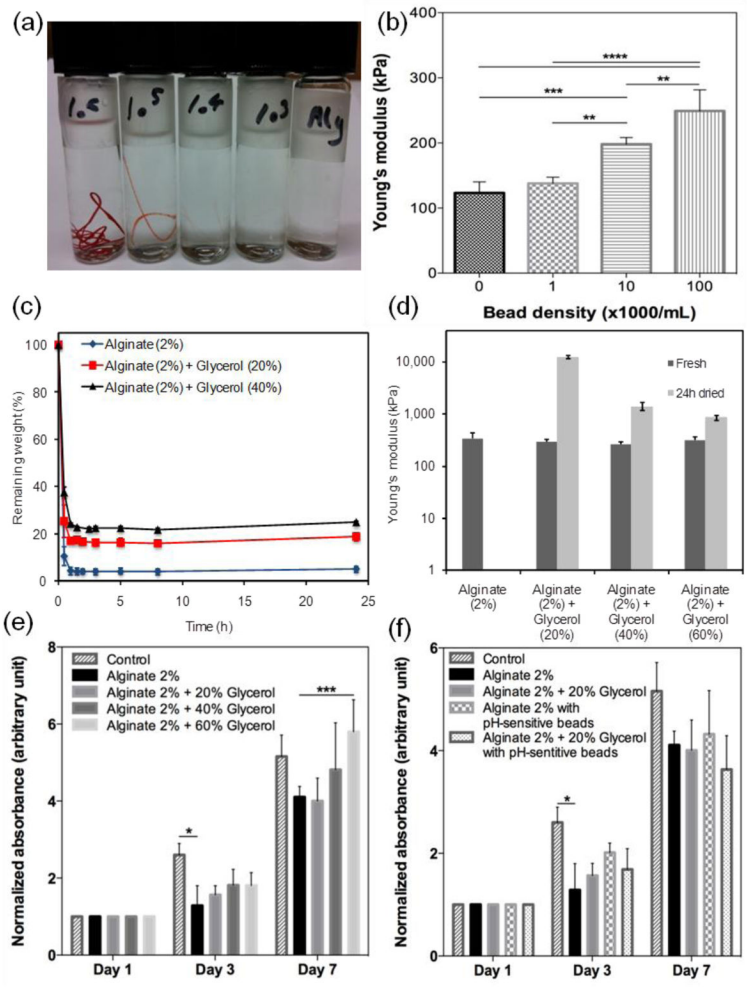

Figure 2.

Physical characterization of the pH-sensing fibers. (a) Visual appearance of fibers with various bead densities; from right to left: 0, 1×10^3, 1×10^4, 1×10^5, 1×10^6. (b) Variation of fiber mechanical strength as a function of bead concentration. (c) Effect of glycerol concentration on the dehydration rate of hydrogels. (d) Variation of fiber mechanical properties immediately after fabrication and after 24 hr dehydration at 37 °C. Metabolic activity of cells cultured with hydrogels containing various (e) glycerol and (f) bead concentrations.

Author Manuscript Author Manuscript Author Manuscript Author Manuscript

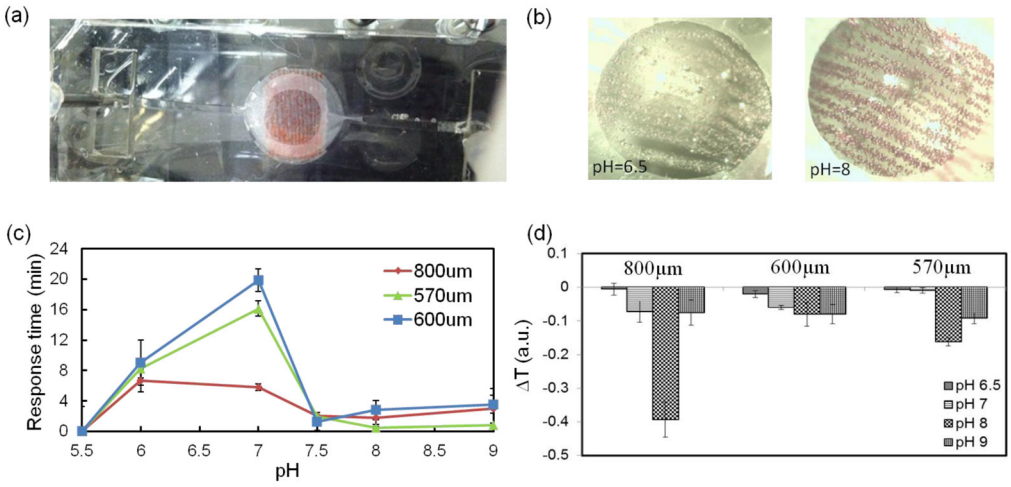

Figure 3.

UV-VIS-NIR USB spectrometer data of the response of the fabricated fiber to pH variation. (a) array of aligned fibers composed of brilliant yellow doped microbeads were placed in a polydimethylsiloxane (PDMS) chamber and exposed to different pH environments. (b) different colors of the pH-responsive fibers at solutions with pH values of 6.5 (yellow) and 8 (red). (c, d) Variation of the response time and detection signal as a function of fiber diameter and different pH environments, respectively.

Author Manuscript Author Manuscript Author Manuscript Author Manuscript

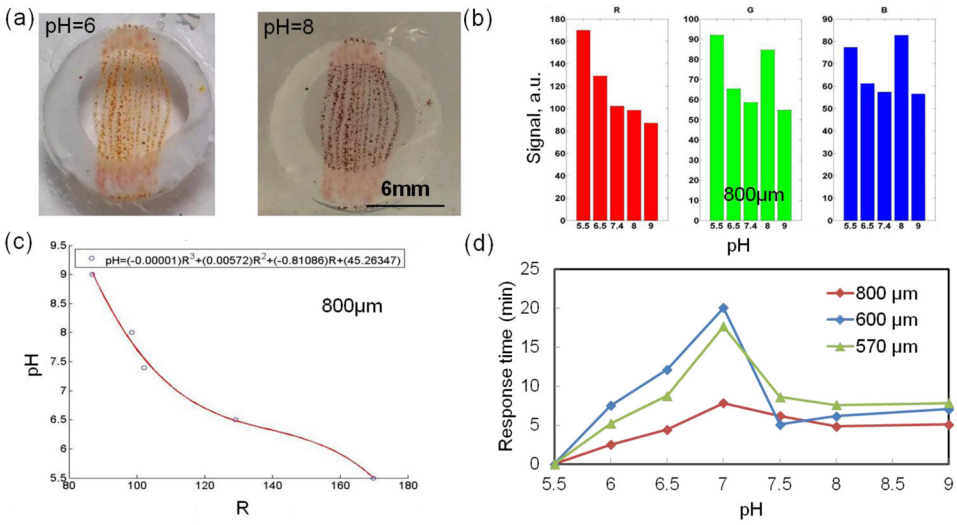

Figure 4.

Data obtained using a smart phone indicating the response of fibers to pH variation. (a) Array of aligned fibers composed of brilliant yellow doped microbeads at different pH environments. (b) Representative example of iPhone signal (RGB) at different pH environments. The responses of sensor arrays based on 800μm aligned fibers composed of microbeads doped with brilliant yellow. (c) pH formula calculated from the RGB signal in (b); (d) Variation of the response time as a function of fiber diameter.

Author Manuscript Author Manuscript Author Manuscript Author Manuscript

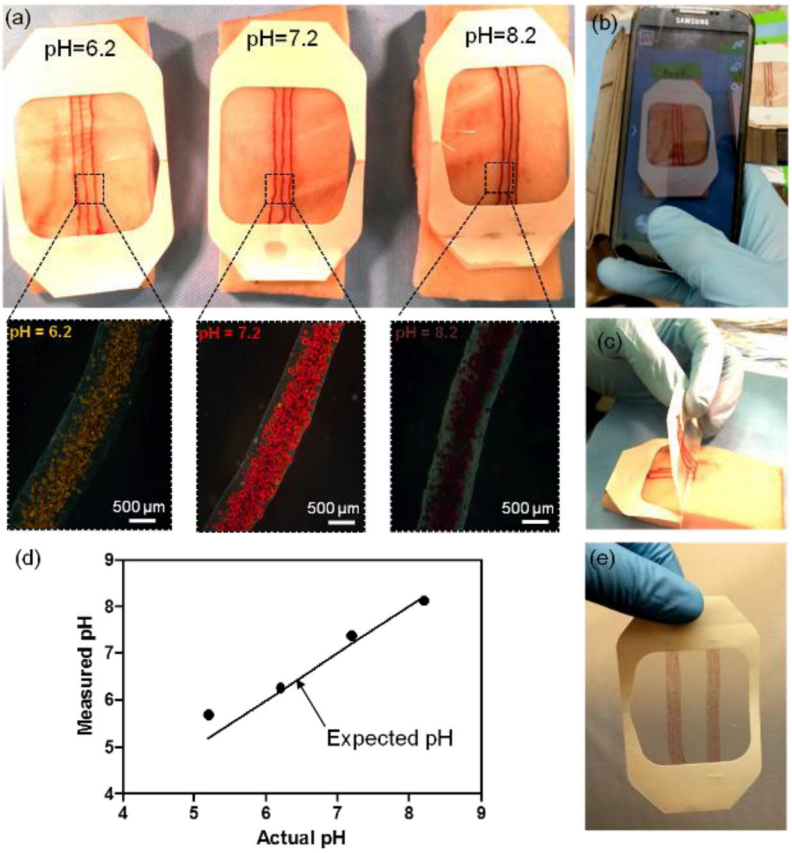

Figure 5.

Fabrication of a pH sensitive wound dressing. (a) Fabricated wound dressings are placed on pieces of pig skin sprayed with solutions of different pH. The images confirm sufficient visual difference for identifying the variation in the skin pH for the range relevant to the values in chronic wounds. The insets are showing the micrographs of the engineered fibers in the corresponding solutions. (b) Taking pictures using smart phone for determining the substrate pH value. (c) Flexibility of the fabricated wound dressing and capability for forming conformal contact with skin. (d) Plot indicating the value of skin pH measured from pictures taken by a smart phone versus the actual pH value of sprayed solutions. (e) A wound dressing fabricated with a stack of smaller diameter fibers to increase the coverage area and facilitate its visual inspection.